

## CLINICAL AND POPULATION STUDIES

### Perivascular Adipose Tissue Inflammation in Ischemic Heart Disease

Celestina Mazzotta, Sanchita Basu, Adam C. Gower, Shakun Karki<sup>1</sup>, Melissa G. Farb, Emily Sroczynski, Elaina Zizza, Anas Sarhan, Ashvin N. Pande, Kenneth Walsh<sup>2</sup>, Nikola Dobrilovic<sup>3</sup>, Noyan Gokce<sup>4</sup>

**OBJECTIVE:** There is growing recognition that adipose tissue–derived proatherogenic mediators contribute to obesity-related cardiovascular disease. We sought to characterize regional differences in perivascular adipose tissue (PVAT) phenotype in relation to atherosclerosis susceptibility.

**APPROACH AND RESULTS:** We examined thoracic PVAT samples in 34 subjects (body mass index  $32 \pm 6$  kg/m<sup>2</sup>, age  $59 \pm 11$  years) undergoing valvular, aortic, or coronary artery bypass graft surgeries and performed transcriptomic characterization using whole-genome expression profiling and quantitative polymerase chain reaction analyses. We identified a highly inflamed region of PVAT surrounding the human aortic root in close proximity to coronary takeoff and adjoining epicardial fat. In subjects undergoing coronary artery bypass graft, we found 300 genes significantly upregulated (false discovery rate  $Q < 0.1$ ) in paired samples of PVAT surrounding the aortic root compared with nonatherosclerotic left internal mammary artery. Genes encoding proteins mechanistically implicated in atherogenesis were enriched in aortic PVAT consisting of signaling pathways linked to inflammation, WNT (wingless-related integration site) signaling, matrix remodeling, coagulation, and angiogenesis. Overexpression of several proatherogenic transcripts, including *IL1 $\beta$* , *CCL2 (MCP-1)*, and *IL6*, were confirmed by quantitative polymerase chain reaction and significantly bolstered in coronary artery disease subjects. Angiographic coronary artery disease burden quantified by the Gensini score positively correlated with the expression of inflammatory genes in PVAT. Moreover, periaortic adipose inflammation was markedly higher in obese subjects with striking upregulation ( $\approx 8$ -fold) of *IL1 $\beta$*  expression compared to nonobese individuals.

**CONCLUSIONS:** Proatherogenic mediators that originate from dysfunctional PVAT may contribute to vascular disease mechanisms in human vessels. Moreover, PVAT may adopt detrimental properties under obese conditions that play a key role in the pathophysiology of ischemic heart disease.

**GRAPHIC ABSTRACT:** A [graphic abstract](#) is available for this article.

**Key Words:** adipose tissue ■ coronary artery disease ■ inflammation ■ interleukin ■ obesity

Obesity is a major cardiovascular risk factor and the accumulation of ectopic and visceral fat, in particular, has been strongly implicated in the pathogenesis of cardiovascular disease.<sup>1,2</sup> Associated risk factors, such as hypertension, diabetes, and hyperlipidemia, only partly explain disease pathophysiology, and mechanisms by which obesity heightens vascular risk are incompletely understood.<sup>3</sup> Perivascular adipose tissue (PVAT) is increasingly gaining attention as a local modulator of vascular function with endocrine and paracrine functions that regulate vascular biology.<sup>4</sup> Although

nearly all human blood vessels are surrounded by PVAT, a potential pathogenic role of PVAT dysfunction in obesity and other conditions has received relatively little attention. In particular, inflammatory cross-talk between PVAT and vascular layers has been proposed to contribute to the pathogenesis of atherosclerosis, but the properties of PVAT in human conduit vessels are largely unexplored.<sup>5,6</sup> The goals of this study were to perform transcriptome based investigations of atherosclerosis-prone and atherosclerosis-resistant human blood vessels and to compare regional differences in perivascular

Correspondence to: Noyan Gokce, MD, Boston Medical Center, 72 E-Concord St, D8, Cardiology Section, Boston, MA 02118. Email [noyan.gokce@bmc.org](mailto:noyan.gokce@bmc.org)

The Data Supplement is available with this article at <https://www.ahajournals.org/doi/suppl/10.1161/ATVBAHA.120.315865>.

For Sources of Funding and Disclosures, see page 1248.

© 2021 American Heart Association, Inc.

*Arterioscler Thromb Vasc Biol* is available at [www.ahajournals.org/journal/atvb](http://www.ahajournals.org/journal/atvb)

## Nonstandard Abbreviations and Acronyms

<b>CAD</b>	coronary artery disease
<b>FDR</b>	false discovery rate
<b>IL</b>	interleukin
<b>LIMA</b>	left internal mammary artery
<b>MCP-1</b>	monocyte chemoattractant protein-1
<b>NFκB</b>	nuclear factor κB
<b>PCR</b>	polymerase chain reaction
<b>PVAT</b>	perivascular adipose tissue
<b>TNF</b>	tumor necrosis factor

adipose phenotype in subjects with obesity and coronary artery disease.

## METHODS

### Study Subjects

Consecutive men and women undergoing elective cardiothoracic surgery at Boston Medical Center were recruited into the study. Surgeries were coronary artery bypass graft ( $n=29$ ), aortic valve replacement ( $n=3$ ), mitral valve replacement ( $n=1$ ), and ascending aortic aneurysm repair ( $n=1$ ). Adipose tissue specimens were collected from thoracic (presteral) subcutaneous fat, anterior pericardium, and proximal ascending aorta, and subjects undergoing coronary artery bypass graft additionally provided distal left internal mammary artery (LIMA) samples. Specimens were procured using scissors rather than electrocautery to avoid thermal tissue damage. Subjects undergoing non-coronary artery bypass graft surgeries ( $n=5$ ) all had nonobstructive coronary artery disease (CAD) by angiography. Pregnant individuals were not eligible for surgery and thus excluded. Preoperatively, clinical characteristics, including body mass index and cardiovascular risk factors, were recorded, and plasma lipid analyses were performed by the Boston Medical Center clinical chemistry laboratory. Left ventricular ejection fraction was derived from clinical echocardiograms. Cross-sectional histology of the LIMA was performed following formalin fixation. After deparaffinization and rehydration, arterial sections were stained with hematoxylin and eosin. The study was approved by the Boston University Medical Center Institutional Review Board and written consent was obtained from all participants.

### Microarray Gene Expression Analysis

Affymetrix GeneChip Human Gene 2.0 ST arrays (Thermo Fisher, Waltham, MA) were used to profile gene expression in total RNA isolated from paired samples of peri-LIMA and peri-aortic fat from 5 subjects with CAD. The probe set mapping interrogates a total of 29635 human Entrez Genes. Arrays were normalized to produce gene-level expression values using the Robust Multiarray Average with the affy-R-package (version 1.58.0) and Entrez Gene-specific R-packages (version 23.0.0) from the Molecular and Behavioral Neuroscience Institute (Brainarray) at the University of Michigan. Differential

## Highlights

- We describe perivascular adipose tissue regional heterogeneity in proatherogenic gene expression of atherosclerosis-prone and atherosclerosis-resistant human thoracic blood vessels.
- Proinflammatory transcripts encoding for proteins mechanistically implicated in atherogenesis were markedly upregulated in the perivascular adipose tissue of individuals with obesity and coronary artery disease.
- Local actions of perivascular adipose tissue may contribute to vascular pathologies in conditions associated with obesity-related adipose tissue dysfunction and ischemic heart disease.

expression was assessed using a paired empirical Bayesian (moderated)  $t$  test as implemented in the limma R package (version 3.38.3). All analyses were performed using the R environment for statistical computing (version 3.5.1). Correction for multiple hypothesis testing was accomplished using the Benjamini-Hochberg false discovery rate (FDR), performed across the genes that were expressed above the median value of at least 5 arrays. Gene Set Enrichment Analysis (version 2.2.1) was used to perform a preranked analysis (default parameters with random seed 1234), ranking the Entrez Gene identifiers of all genes interrogated by the array according to the paired moderated  $t$  statistic, and using the Entrez Gene versions of the Hallmark, c2 (Biocarta, KEGG [Kyoto Encyclopedia of Genes and Genomes], and Reactome only), c5 (Gene Ontology), and c3 (transcription factor and microRNA motif) collections of gene sets obtained from the Molecular Signatures Database (MSigDB), version 6.0. All raw and processed data have been made publicly available and deposited into the Gene Expression Omnibus repository (Series GSE152326). All microarray procedures and analyses were carried out by the Boston University Microarray and Sequencing Resource.

### Gene Expression Analysis Using Quantitative Polymerase Chain Reaction

Adipose tissue samples were collected in All Protect Reagent (Qiagen) and stored at  $-80^{\circ}\text{C}$ . Total mRNA was isolated using the RNeasy Lipid Tissue Mini Kit (Qiagen), and RNA concentration was measured using a Thermo Fisher Nanodrop 2000 at 260/280 nm. Two hundred nanograms of RNA were reverse transcribed into cDNA using a High Capacity cDNA Reverse Transcription Kit (Applied Biosystems). TaqMan PreAmp Master Mix and TaqMan gene expression assays (Applied Biosystems) were used for a preamplification step of selected target genes, using a T100 Thermal Cycler (Bio-Rad). The PreAmp samples were diluted 1:20 using DNase- and RNase-free water and stored at  $-20^{\circ}\text{C}$  until use. The real-time polymerase chain reaction (PCR) of glyceraldehyde-3-phosphate dehydrogenase (*GAPDH*), WNT (wingless-related integration site) family member 5A (*WNT5A* [Wnt family member 5a]), receptor tyrosine kinase-like orphan receptor 1 (*ROR1*), receptor

**Table 1. Probes for qPCR**

Gene symbol	Assay ID	Entrez gene ID
<i>GAPDH</i>	Hs02758991_G1	2597
<i>WNT5A</i>	Hs00998537_m1	7474
<i>ROR1</i>	Hs00938677_m1	4919
<i>ROR2</i>	Hs00896176_m1	4920
<i>VANGL2</i>	Hs00393412_m1	57216
<i>PRICKLE1</i>	Hs01055551_m1	144165
<i>IL1<math>\beta</math></i>	Hs01555410_m1	3553
<i>CCL8</i>	Hs04187715_m1	6355
<i>CCL2</i>	Hs00234140_m1	6347
<i>IL6</i>	Hs00174131_m1	3569
<i>MAPK8 (JNK)</i>	Hs01548508_m1	5599

qPCR indicates quantitative polymerase chain reaction.

tyrosine kinase–like orphan receptor 2 (*ROR2*), planar cell polarity protein 2 (*VANGL2*), interleukin 1 $\beta$  (*IL1 $\beta$* ), C-C motif chemokine ligand 2 (*CCL2*), C-C motif chemokine ligand 8 (*CCL8*), interleukin 6 (*IL6*), and mitogen-activated protein kinase 8 (*MAPK8*), (Table 1) were performed with a Viia7 thermal cycler (Applied Biosystems), using TaqMan gene expression assays and TaqMan Gene Expression Master Mix, with *GAPDH* as the housekeeping gene. Expression data for all target genes were normalized to *GAPDH*, analyzed using the  $\Delta\Delta C_t$  method, and expressed as fold difference of aortic compared with LIMA PVAT.

## Western Immunoblot Analyses

Proteins were extracted from adipose tissue by homogenization in liquid nitrogen and 1X lysis buffer (Cell Signaling, Danvers, MA) supplemented with protease and phosphatase inhibitor cocktail (Sigma Aldrich, St. Louis, MO). Twenty micrograms of total protein was subjected to electrophoresis using sodium dodecyl sulfate (SDS)–polyacrylamide gel and blotted to nitrocellulose membranes. The membranes were blocked then washed with TBS and incubated overnight at 4°C with the following primary antibodies: monoclonal mouse anti-human UCP-1 (uncoupling protein-1; 1:500 dilution, R&D Systems, MN), polyclonal rabbit anti-human CCL2 (1:500 dilution, LS-BIO, WA), mouse monoclonal anti-human IL6 (1:500 dilution, LS-BIO, WA), and monoclonal mouse anti-human  $\beta$ -actin (1:5000 dilution; Sigma, St Louis, MO), washed, and incubated on a rotary shaker at room temperature for 90 minutes with appropriate HRP (horseradish peroxidase)-conjugated secondary antibody. After washing, immune complexes were detected by enhanced chemiluminescence (Pierce, Rockford, IL). Protein levels were quantified using Image J software and values were normalized to  $\beta$ -actin.

## Adipocyte Sizing

Paired samples of peri-LIMA and periaortic adipose tissue from 5 subjects with CAD were stained using standard hematoxylin and eosin, and images captured using a color digital camera attached to a microscope at  $\times 10$  to  $\times 40$ . For each tissue section, adipocyte size (diameter,  $\mu\text{m}$ ) was quantified using Adiposoft version 1.16 (advanced distribution of Image J) by a blinded individual.<sup>7</sup>

## Gensini Quantitative Angiography Score

Coronary artery disease severity was assessed using quantitative coronary angiography software (Philips, Netherlands), using established scoring systems by a single interventional cardiologist blinded to all adipose tissue and clinical data. The modified Gensini score was used to characterize the angiographic burden of CAD.<sup>8,9</sup> In this model, each identified lesion was assigned a percentage diameter stenosis by quantitative coronary angiography, then assigned a score (1 for 0%–25% stenosis, 2 for 26%–50%, 4 for 51%–75%, 8 for 76%–90%, 16 for 91%–99%, and 32 for 100%). If the lesion was  $\geq 99\%$ , a modifier was considered based on collaterals and atherosclerotic burden in the source vessel. A prespecified multiplier was assigned to each segment depending on location of the lesion (5 for left main coronary artery, 2.5 for proximal left anterior descending and proximal left circumflex branches, 1.5 for midsegment of left anterior descending artery, 0.5 for second diagonal branch and posterolateral branch, and 1 for other branches). The modified Gensini score was reported for each participant as a sum of these weighted scores with higher scores indicating more severe CAD.

## Statistical Analysis

Data are expressed as the mean $\pm$ SD in tables. Student paired *t* test was used to compare within-subject differences in adipose tissue gene expression. Nonparametric tests were used to compare group differences in mRNA transcripts and protein expression that were non-normally distributed, as assessed by Kolmogorov-Smirnov methodology. Spearman correlations were used for analyses of Gensini scores with gene expression. Graphic data are presented as mean $\pm$ SEM unless otherwise indicated. A value of  $P < 0.05$  was considered significant for all analyses.

## RESULTS

### Clinical Characteristics

A total of 34 subjects were recruited for the study. Clinical characteristics of all subjects are displayed in Table 2. Consistent with cardiac surgery populations, there was a predominance of cardiovascular risk factors and obesity. Surgeries consisted of coronary artery bypass graft ( $n=29$ ), aortic valve replacement ( $n=3$ ), mitral valve replacement ( $n=1$ ), and ascending aortic aneurysm repair ( $n=1$ ). In these subjects, there was high prevalence of statin use (94%) with mean plasma LDL-C (low-density lipoprotein cholesterol)  $\leq 90$  mg/dL.

### Adipose Tissue Sampling

We collected adipose tissue samples from thoracic subcutaneous, anterior pericardial, proximal periaortic, and distal LIMA regions. Exploratory gene expression analyses demonstrated the largest differences between the latter 2 sample sites, which were thus used for subsequent analyses. A representative image of the surgical field where periaortic specimens were taken is



**Table 2. Clinical Characteristics of the Study Population**

Parameter	N=34
Age, y	59±11
Sex, M, (%)	76
Weight, kg	98±22
BMI, kg/m <sup>2</sup>	32±6
Obese, %	65
Total cholesterol, mg/dL	168±48
LDL cholesterol, mg/dL	90±41
HDL cholesterol, mg/dL	43±20
Triglycerides, mg/dL	142±72
Statin medication use, %	94
Hypertension, %	85
Coronary artery disease, %	85
Diabetes, %	35
Angiographic Gensini score	67±32
Left ventricular ejection fraction, %	50±14

Data are mean±SD. BMI indicates body mass index; HDL, high-density lipoprotein; and LDL, low-density lipoprotein.

displayed in Figure 1. We used histology to examine cross-sections of the distal LIMA (near touchdown site) and confirmed absence of atherosclerotic plaques as displayed in Figure 2A and 2B. Therefore, LIMA PVAT specimens were used as control samples in subsequent gene expression analyses. We performed adipocyte sizing of paired PVAT samples in 5 subjects with CAD and observed no difference in adipocyte diameter between LIMA (Figure 2C) compared with aortic (Figure 2D) PVAT (54±9 μm versus 69±19 μm, respectively, *P*=0.14).

**Differential Microarray Expression Analysis Between Aortic and LIMA PVAT**

We used whole-genome microarrays to profile gene expression in total RNA obtained from PVAT of 5 male subjects with CAD (age 60±5 years, 80% obese, mean LDL-C 89±31 mg/dL, 100% statin use). Each subject provided paired PVAT samples from both the aortic root and LIMA simultaneously, thus avoiding confounding influence from systemic variables and sex. A total of 324 genes were significantly differentially expressed between depots (FDR *Q*<0.1), with 300 genes upregulated and 24 genes downregulated in aortic PVAT compared with that from LIMA. The relative transcriptional signature and gene patterning were remarkably consistent for each subject. Genes that were upregulated in aortic PVAT included transcripts associated with inflammasomes (*NLRP3*), TNF (tumor necrosis factor) α signaling (*TNFAIP2*, *TNFAIP3*, *TNFSF8*, *TNFRSF1A*, and *TNFRSF10D*), IL1 signaling (*IL1R1*, *IRAK3*), IL6 signaling (*IL6*), NFκB (nuclear factor κB) signaling (*NFKB1*), leukocyte adhesion (*VCAM1*), macrophage chemotaxis (*CCL2/MCP-1*), and chemokine signaling (*CXCL16*, *CCL21*, *CCL13*). The complete set of statistical analysis results is provided in File I in the [Data Supplement](#).

We then performed Gene Set Enrichment Analysis to identify pathways and biological processes that were coordinately upregulated in aortic PVAT compared with the LIMA. A high number of gene sets were significantly coordinately upregulated (FDR *Q*<0.01), including those corresponding to the Gene Ontology (GO) biological process terms “positive regulation of inflammatory response” (GO:0050729, FDR *Q*<0.001), “cellular response to

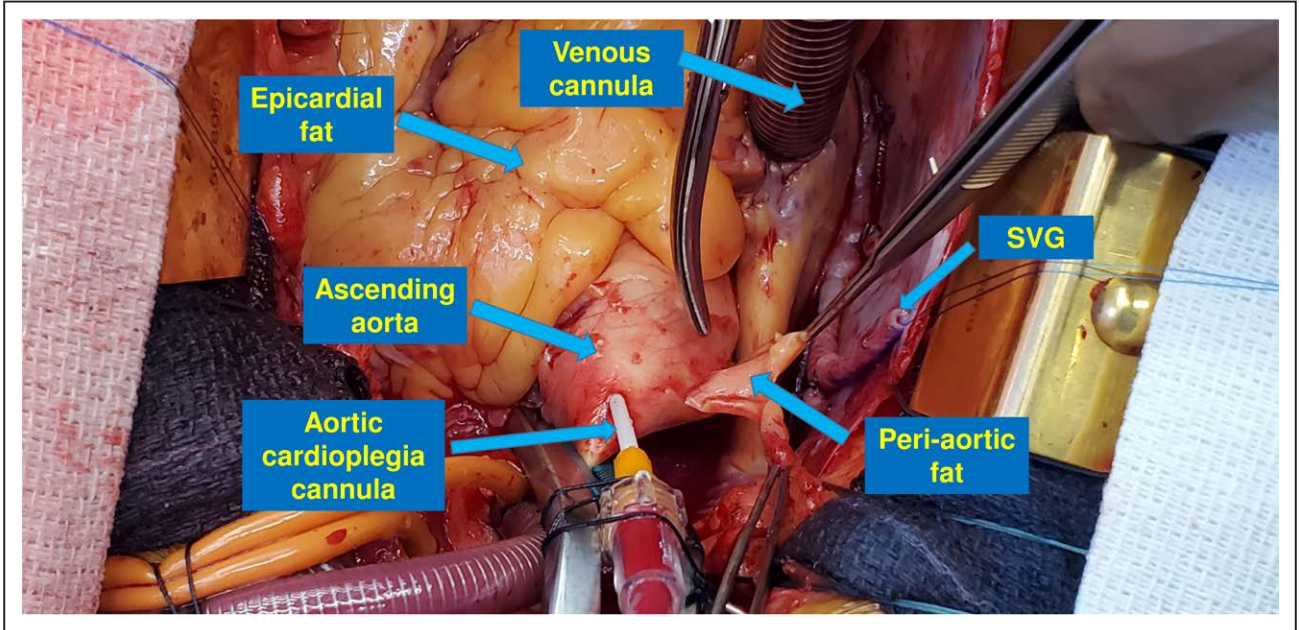


**Figure 1. Representative operative field during coronary artery bypass graft surgery in an obese subject demonstrating extensive adipose tissue accumulation surrounding cardiovascular territories.** SVG indicates saphenous venous graft.

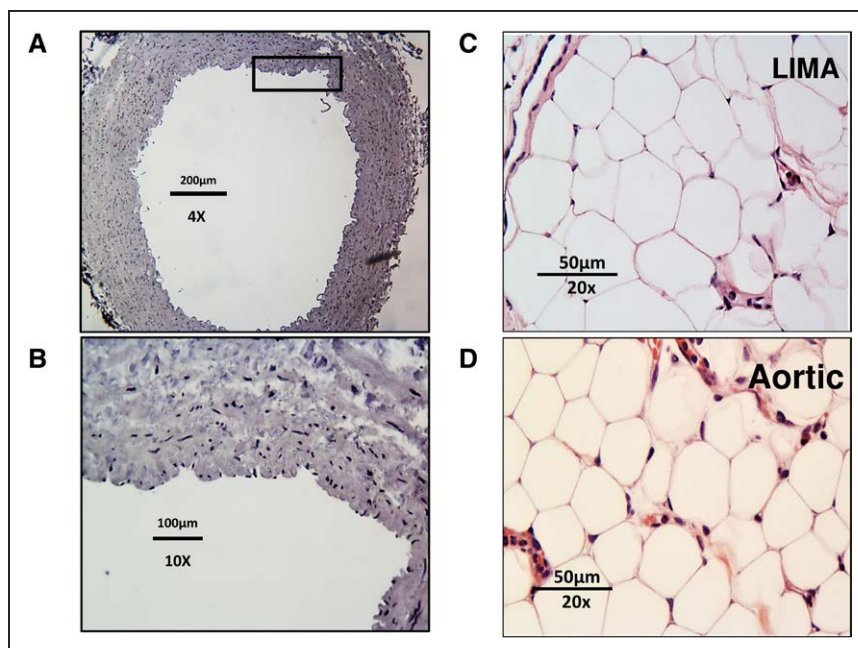


**Figure 2. Histological analyses.**

Cross-sectional hematoxylin staining of the left internal mammary artery (LIMA) demonstrating no visible plaques as shown in (A) upper panel 4x and (B) lower panel 10x magnification. Representative histology of paired perivascular adipose tissue samples from (C) LIMA and (D) aortic specimens (20x magnification). There was no significant difference in adipocyte morphology or size between the 2 depots.

interleukin-1" (GO:0071347, FDR  $Q < 0.001$ ), "positive regulation of interleukin-1 production" (GO:0032732, FDR  $Q = 0.0057$ ), "cellular response to interleukin-6" (GO:0071354, FDR  $Q < 0.001$ ); "leukocyte chemotaxis" (GO:0030595, FDR  $Q < 0.001$ ), and "noncanonical Wnt signaling pathway" (GO:0035567, FDR  $Q = 0.0057$ ); the BioCarta IL1R pathway (FDR  $Q < 0.001$ ), and the KEGG adipocytokine signaling pathway (hsa04920, FDR  $Q = 0.0048$ ). A heatmap of the expression of the combined set of leading-edge genes of these results (ie, those genes that contributed most to the significance of each result) is shown in Figure 3. A complete set of Gene Set Enrichment Analysis results is provided in File II in the [Data Supplement](#).

### Quantitative PCR and Western Immunoblot Analyses

We then selected several genes of interest from the microarray analysis for confirmatory quantitative PCR in a larger cohort of subjects. These candidates included genes that were relevant to atherosclerosis and significantly upregulated in aortic PVAT (*CCL2*, FDR  $Q = 0.064$ ; *CCL8*, FDR  $Q = 0.12$ ; *IL1B*, FDR  $Q = 0.12$ ; *IL6*, FDR  $Q = 0.06$ ; *ROR1*, FDR  $Q = 0.19$ ), as well as others that were not nominally significant ( $P > 0.05$ ) but were included in the leading edge of at least one gene set with a significant Gene Set Enrichment Analysis result (*MAPK8/JNK*, *WNT5A*; see Figure 3) or have been previously implicated in obesity and cardiovascular disease (*ROR2*).<sup>10,11</sup> As shown in Figure 4, these genes were significantly upregulated in aortic compared with LIMA PVAT. For protein confirmation, we then performed Western immunoblot analyses for IL6 and CCL2 and demonstrated significant upregulation in aortic PVAT

(Figure 5) firmly mirroring gene expression data. In contrast, UCP-1 expression as a marker for distinguishing white/beige/brown fat phenotypes<sup>12,13</sup> was not differentially expressed between these 2 depots ( $P = \text{nonsignificant}$ ). Furthermore, we observed significant upregulation of proinflammatory transcripts (*IL1B*, *CCL2*, *CCL8*, *IL6*, *MAPK8/JNK*) and genes involved in noncanonical Wnt signaling (*ROR2*, *VANGL2*, prickle planar cell polarity protein-1 [*PRICKLE1*]) in the aortic PVAT of obese subjects (body mass index  $\geq 30$  kg/m<sup>2</sup>) relative to nonobese subjects (Figure 6) and in inflammatory genes in subjects with CAD versus those without CAD (Figure 7). Additional subanalyses excluding all subjects without CAD still showed significant upregulated expression of *IL1B*, *PRICKLE1*, *CCL2*, and *IL6* ( $P < 0.05$  for all) in the aortic PVAT of obese compared with nonobese subjects. Finally, we found that the expression of both *CCL2* (*MCP-1*) and *IL6* in aortic PVAT significantly correlated with angiographic Gensini score, a measure of the extent of CAD (Figure 8), in this group of individuals who had a high prevalence of statin use and relatively good LDL-C control ( $\leq 90$  mg/dL).

### DISCUSSION

In the present study, we demonstrate transcriptional upregulation of a broad range of proatherogenic mediators in the PVAT of subjects with coronary artery disease. Even with a small sample size, microarray analyses showed strong concordance across subjects with significant upregulation of at least 300 genes, many of which are mechanistically implicated in cardiovascular disease. We also describe for the first time, to our knowledge, that the expression of specific proinflammatory transcripts was significantly increased in the PVAT of

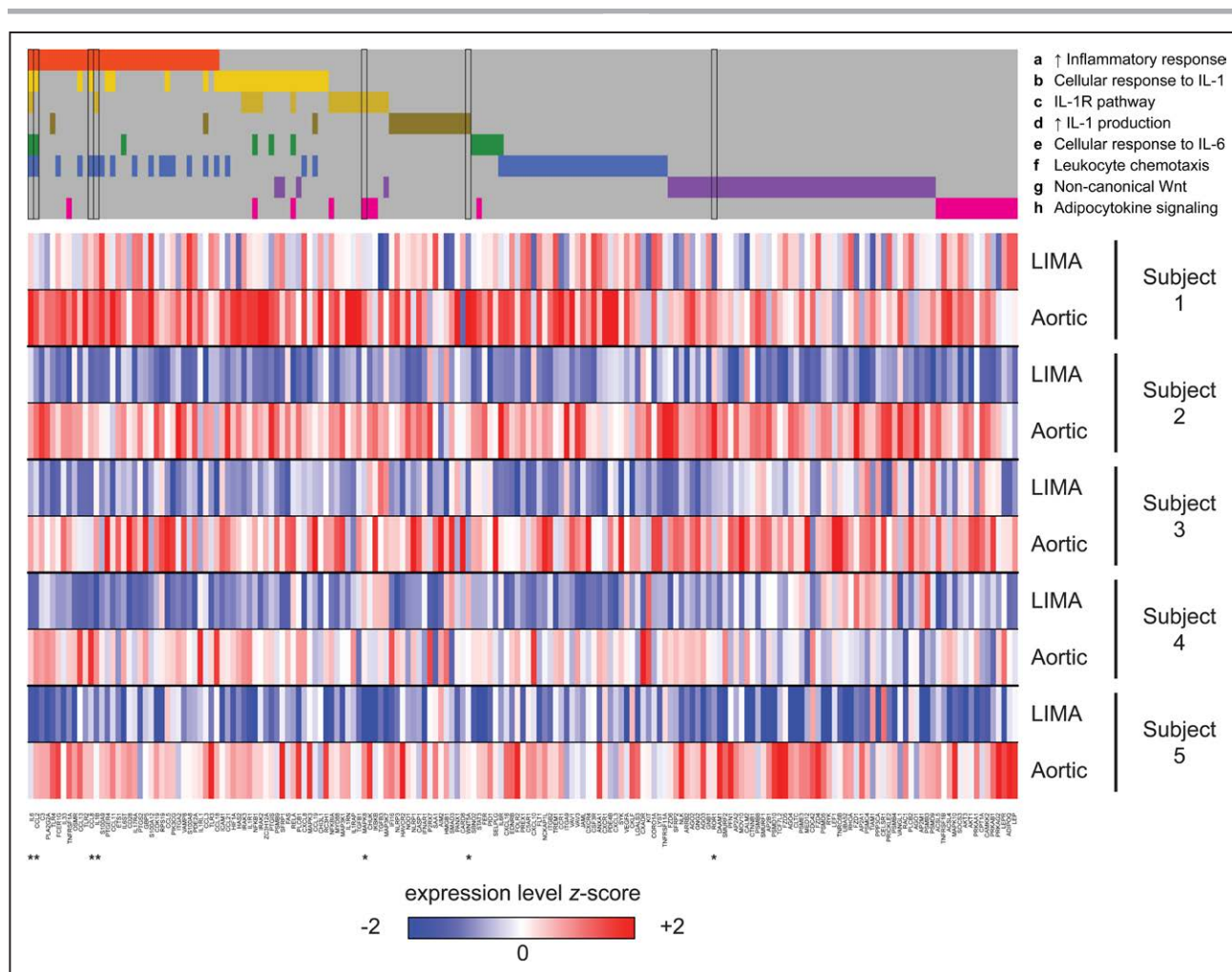


**Figure 3. Heatmap of the union set of leading-edge genes from 8 selected gene sets with significant coordinate upregulation (false discovery rate  $Q < 0.01$ ) in aortic vs left internal mammary artery (LIMA) perivascular adipose tissue.**

The membership of each gene within each gene set is indicated with a colored box at the top of the heatmap: (a) Gene Ontology (GO) term “positive regulation of inflammatory response”; (b) GO term “cellular response to interleukin-1”; (c) BioCarta IL1R pathway; (d) GO term “positive regulation of interleukin-1 production”; (e) GO term “cellular response to interleukin-6”; (f) GO term “leukocyte chemotaxis”; (g) GO term “noncanonical Wnt (wingless-related integration site) signaling pathway”; (h) KEGG (Kyoto Encyclopedia of Genes and Genomes) adipocytokine signaling pathway. Rows and columns correspond to samples and genes, respectively. Columns are sorted in left to right first by gene set and then by moderated  $t$  statistic. Gene expression values were Z score-normalized to a mean of zero and SD of 1 across all samples in each column, with blue, white, and red indicating final Z scores of  $\leq -2$ , 0, and  $\geq 2$ , respectively. Genes selected for subsequent quantitative polymerase chain reaction analyses are indicated with asterisks next to each gene symbol below the heatmap and black boxes above the heatmap. IL indicates interleukin.

subjects with obesity or CAD and correlated positively with angiographic atherosclerotic burden. These findings were observed in a group with relatively well-controlled LDL-C levels and high prevalence of statin use, evoking the notion of residual inflammatory cardiovascular risk in many individuals.<sup>5</sup> Collectively, these data provide basis for a potential role of PVAT dysregulation contributing to the pathogenesis of atherosclerosis.

Vascular inflammation plays a key role in all phases of atherosclerosis,<sup>14</sup> and there is growing recognition that PVAT can participate in this process.<sup>3</sup> Nearly all human conduit vessels are surrounded by adipose tissue coatings that contain a mixture of cell types including adipocytes, stem cells, immune cells, and nervous tissue that juxtapose with the adventitial vasa vasorum

and communicate bidirectionally with all vascular layers. Although PVAT functions are largely homeostatic,<sup>6,15–18</sup> perturbations can develop in obesity and other conditions that support pathological rather than protective roles for PVAT.<sup>3,19</sup> Traditional concepts of vascular inflammation have evolved beyond the classic inside-out monocyte adhesion and lipid oxidation paradigms that begin at the endothelial surface. In fact, there are growing animal<sup>20</sup> and human<sup>21,22</sup> data supporting a parallel outside-in inflammatory process initiated externally that can propagate inward.<sup>23</sup> In this regard, the adventitia elaborates a range of chemokines and cytokines that regulate neovascularization, vascular tone, and angiogenesis<sup>17,24</sup> and can function as major sites of immune cell accumulation that influence plaque



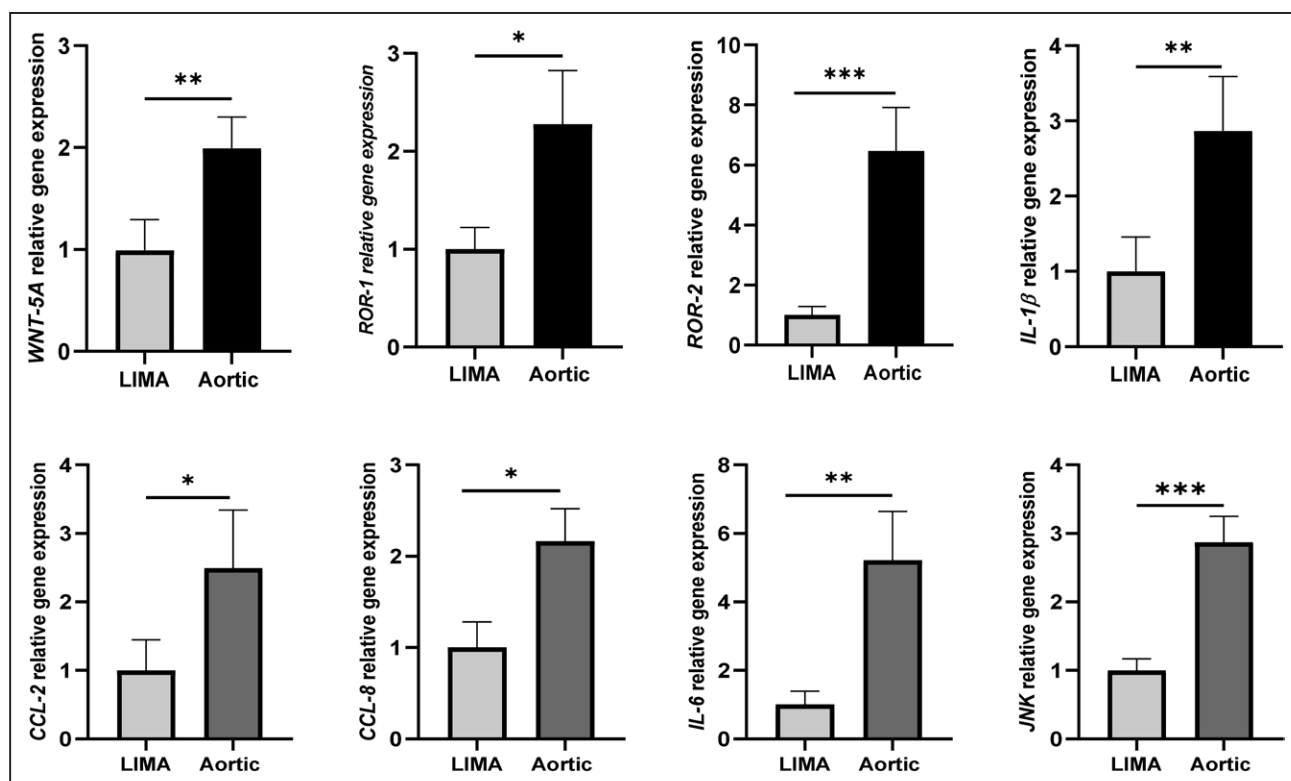


**Figure 4. Expression of *WNT5A* (Wnt family member 5a) signaling and proinflammatory genes is significantly upregulated in aortic compared to left internal mammary artery (LIMA) perivascular adipose tissue.**

Data are expressed as fold difference of aortic compared with LIMA (set to 1) depots, performed in triplicates by quantitative polymerase chain reaction and normalized to *GAPDH* gene expression. Paired *t* tests were used for statistical analysis ( $n=20$ ). Data are mean $\pm$ SEM. \* $P<0.05$ , \*\* $P<0.01$ , \*\*\* $P<0.001$ .

pathobiology.<sup>20,23,25–27</sup> Direct causal evidence of a pro-atherogenic role for PVAT comes from experimental animal transplant studies where relocation of pathogenic fat onto recipient carotid vessels promotes atherosclerosis in apoE knockout mice,<sup>28</sup> and transposition of aortic PVAT from obese mice accelerates neointimal hyperplasia and adventitial macrophage infiltration.<sup>29</sup> Human observational studies report that PVAT colocalizes with atherosclerotic plaques<sup>30</sup> and associates with advanced lesions.<sup>31</sup> Several studies focusing on epicardial adipose tissue in patients with CAD describe a more proinflammatory profile compared with subcutaneous fat<sup>32–34</sup> and higher secretion of adipocytokines and monocyte chemotaxis near stenotic coronary segments.<sup>21,35</sup> More compelling data come from recent computer tomography vascular imaging studies which show that quantitative measures of coronary perivascular fat inflammation predict cardiovascular events independent of CAD stenosis and even before the evolution of discernable plaques.<sup>36,37</sup>

Although the mechanisms by which PVAT promotes atherosclerosis progression and instability in humans remain an open question, our comparative data may provide several important clues. It has been long recognized that the internal mammary artery (IMA), which represents a thoracic vessel of similar size and histology

as the coronaries and is exposed to the same systemic risk factors rarely develops atherosclerosis, for largely unknown reasons, and is thus widely used as a bypass conduit. Autopsy studies that compared IMA to coronary specimens have identified the importance of local anatomic factors as determinants of lesion development.<sup>38</sup> One such variable may relate to regional PVAT heterogeneity, yet few comparative studies have specifically examined the cellular composition or adipokine expression of IMA PVAT, and these were mainly cadaveric,<sup>21,39,40</sup> limited to males<sup>41</sup> or nonobese subjects.<sup>42</sup> PVAT surrounding the IMA exerts vasodilatory effects<sup>43</sup> and endothelial cells express higher eNOS (endothelial NO synthase) and atheroprotective genes.<sup>44,45</sup> Moreover, IMA grafts pass this protection onto downstream native target vessels which strongly suggests paracrine signaling.<sup>46</sup> Our global analyses demonstrated a more quiescent IMA phenotype with regard to inflammation, macrophage chemotaxis, cytokine reactome, matrix turnover, and coagulation between depots, raising the possibility that lesser adipose tissue dysfunction around the IMA may be one mechanism explaining the relative protection of this vessel against atherosclerosis. Understanding mechanisms of IMA resistance to atherogenesis may generate new strategies to treat or prevent CHD.

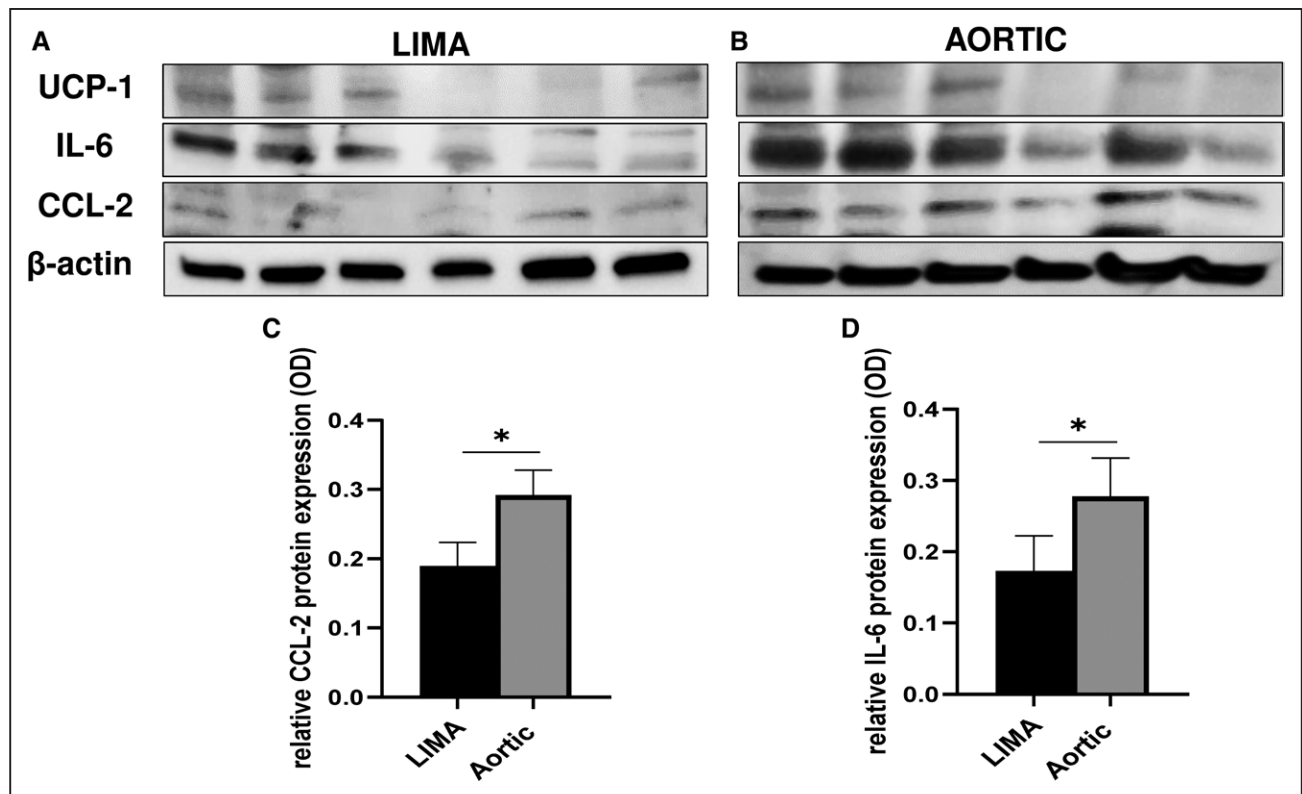


**Figure 5.** Western immunoblot analyses demonstrate significantly increased protein expression of IL (interleukin)-6 and CCL (C-C motif chemokine ligand)-2 in aortic compared to left internal mammary artery (LIMA) perivascular adipose tissue (PVAT) confirming gene expression data.

In contrast, no interdepot PVAT difference in UCP-1 (uncoupling protein-1) protein expression was observed ( $P$ =nonsignificant). Data are expressed as relative protein expression using optical density (OD), normalized to  $\beta$ -actin protein. Wilcoxon rank-sum testing was used for statistical analyses ( $n=5$ ). Data are mean $\pm$ SEM; \* $P<0.05$ .

A novel aspect of our study is our discovery of a regional hub of highly inflamed PVAT surrounding the aortic root in close proximity to coronary takeoff and epicardial fat. This anatomic region frequently referred to as Rindfleisch's folds<sup>47</sup> has received no attention in clinical investigation yet shares vascular

networks contiguous with epicardial and myocardial territories as no distinct anatomic boundaries separate these regions. Moreover, very few studies have compared the characteristics of PVAT in subjects with and without CAD, and published studies with nonobstructive coronaries are extremely rare.<sup>48,49</sup> Reports in

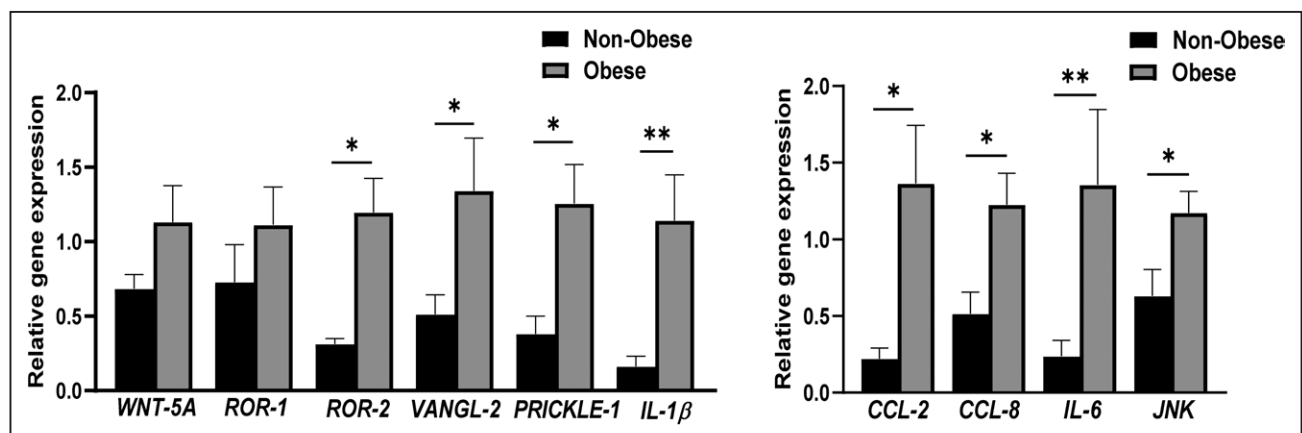


**Figure 6.** Periaortic perivascular adipose tissue expression of proinflammatory transcripts is significantly upregulated in obese compared with nonobese subjects.

Data are expressed as relative gene expression (arbitrary units), performed in triplicates by quantitative polymerase chain reaction, and normalized to *GAPDH* gene expression. Mann-Whitney testing was used for statistical analyses ( $n=17$  obese,  $n=7$  nonobese). Data are mean $\pm$ SEM. \* $P<0.05$ , \*\* $P<0.01$ .



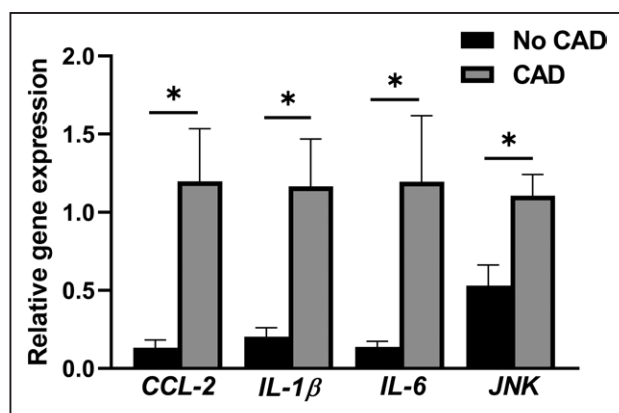


**Figure 7.** Periaortic perivascular adipose tissue expression of proinflammatory transcripts is significantly upregulated in subjects with coronary artery disease (CAD; n=22) compared to individuals without CAD (n=5).

Data are expressed as relative gene expression (arbitrary units), performed in triplicates by quantitative polymerase chain reaction, and normalized to *GAPDH* gene expression. Mann-Whitney testing was used for statistical analyses. Data are mean  $\pm$  SEM. \* $P < 0.05$ .

nonobese patients with CAD showed lower expression of the vasculoprotective factor adiponectin<sup>50</sup> and higher inflammation in epicardial adipose tissue,<sup>49</sup> whereas other studies utilizing microarrays showed few differences<sup>51</sup> and no differential UCP-1 expression.<sup>52</sup> In patients with CAD, we identified significant enrichment in aortic PVAT genes encoding for numerous proteins implicated in atherogenesis including *CCL2/MCP-1*, *CCL8*, *IL1 $\beta$* , and *MAPK8/JNK*, as well as components of noncanonical Wnt pathway signaling<sup>53</sup> not previously highlighted.

Another novel aspect of our study was the ability to examine the influence of obesity on PVAT phenotype, and to our knowledge, no prior study has directly compared gene expression in the aortic PVAT of obese

versus nonobese subjects. A prior swine study reported a greater constrictive effect of coronary PVAT in obese animals,<sup>54</sup> and higher epicardial adipose tissue inflammation was described in CAD subjects with body mass index  $>27$  kg/m<sup>2</sup>.<sup>48</sup> Perivascular fat can adopt detrimental properties under obese conditions that contribute to the pathophysiology of cardiovascular disease<sup>55,56</sup> and severe obesity can fully encase cardiac structures in fat  $\geq 2$  cm thick (*cor adipe plane tectum*).<sup>57</sup> In the Framingham Heart Study, measures of periaortic fat were associated with aortic stiffness and cardiovascular risk.<sup>58,59</sup> In contrast, coronaries lacking adipose coatings in segments bridged by myocardial tissue are protected from atherosclerosis.<sup>60</sup> Thus far, mechanistic evidence for obesity-induced changes in PVAT has largely come from animals. For instance, high-fat-fed mice exhibit impaired periaortic adipocyte differentiation<sup>39</sup> and endothelial vasodilator dysfunction via mechanisms linked to adipose macrophage chemotaxis and oxidative stress.<sup>61</sup> High-fat feeding triggers microRNA conversion that evokes PVAT inflammatory responses and arterial remodeling.<sup>62</sup> In the present study, we observed significant inflammasome upregulation in PVAT associated with obesity, directionally similar to that seen in patients with CAD. In this regard, a chronic state of low-grade inflammation in obesity driven in part by adipose tissue inflammation has been well recognized, and we have previously described the contribution of noncanonical Wnt proinflammatory signaling to mechanisms of insulin resistance and vascular dysfunction.<sup>2,11,63,64</sup> Experimental data suggest that PVAT responds to external factors, highlighting the plasticity of this tissue and its potential for therapeutic modulation. Macrophage ablation restores anticontractile functions of PVAT,<sup>65</sup> and nitric oxide-dependent vasodilation of the microvasculature is restored with weight

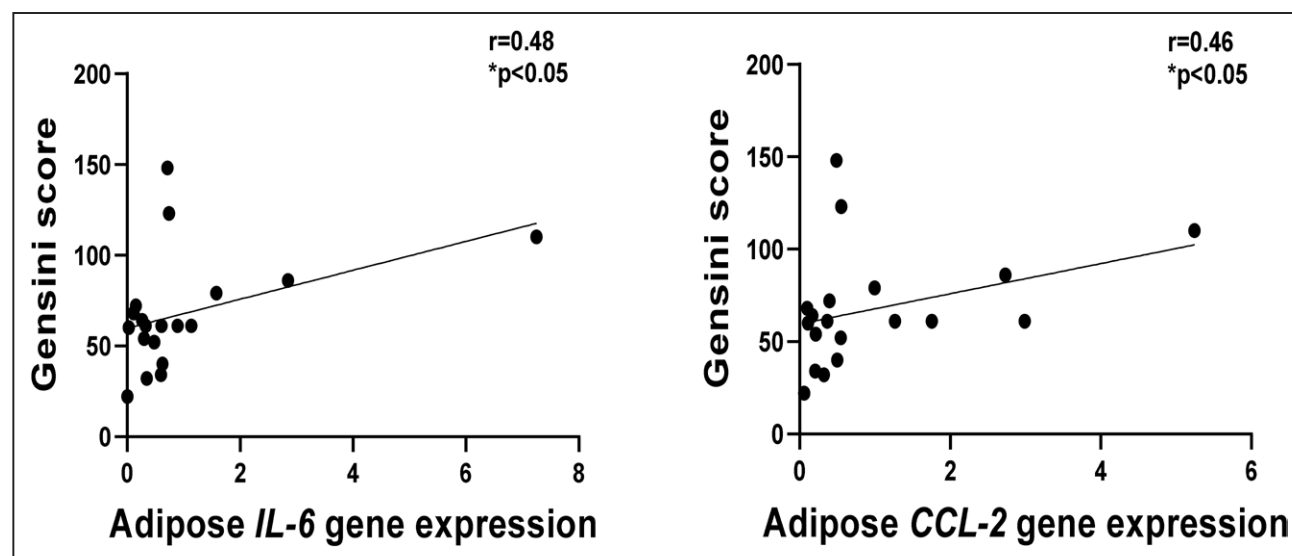


**Figure 8.** Spearman correlations demonstrating significant positive correlations periaortic adipose tissue gene expression of CCL2 (right) and IL6 (left) with cumulative coronary artery disease burden assessed by quantitative angiography Gensini scores (n=19).

loss.<sup>66</sup> Statins modify PVAT in hypertensive rat aortas<sup>67</sup>; however, nothing is known with regard to therapeutic modulation in human disease. Presently, we are only at the beginning of understanding PVAT biology, and future studies are required to characterize its pathogenic role and treatment implications in obesity-related cardiovascular diseases.

## LIMITATIONS

First, the number of subjects was limited but expected with this type of invasive study involving cardiac surgeries. We point out that we utilized freshly isolated samples from living subjects rather than rely on autopsy specimens. Even with a small sample size, the microarray results were strongly significant, and we were able to verify the expression of specific genes by qPCR. Second, we did not have LIMA samples from non-CAD patients since this region is not accessed by the surgeon. Third, unmeasured clinical confounders could influence intergroup differences; however, this was avoided in our microarray study as paired samples were obtained from the same subject. Fourth, the study is observational and does not prove causal relationships; however, our data firmly build upon the scant human literature in the field. Fifth, multidetector-row computer tomography angiography was not available in all subjects to quantify degree of aortic atherosclerosis. Lastly, from a conceptual standpoint, it is possible that PVAT inflammation stems partly from the diseased vessel that extends to surrounding adipose tissue, and although imaging studies suggest this may be otherwise,<sup>36</sup> this concept warrants further mechanistic investigation.

In conclusion, human thoracic PVAT displays marked territorial heterogeneity with distinct overexpression of proatherogenic transcriptional profiles in subjects with obesity and CAD. Local actions of PVAT may contribute to vascular pathologies in conditions associated with obesity-induced adipose tissue dysfunction.

## ARTICLE INFORMATION

Received August 27, 2020; accepted January 13, 2021.

### Affiliations

Evans Department of Medicine and Whitaker Cardiovascular Institute (C.M., S.B., S.K., M.G.F., E.S., E.Z., A.S., A.N.P., N.G.) and Clinical and Translational Science Institute (A.C.G.), Boston University School of Medicine, MA. Hematovascular Biology Center and the Robert M. Berne Cardiovascular Research Center, University of Virginia School of Medicine, Charlottesville (K.W.). Division of Cardiac Surgery, Department of Surgery, Boston Medical Center, MA (N.D.).

### Acknowledgments

We acknowledge their contribution, review, and approval of this article.

### Sources of Funding

Dr Gokce is supported by National Institutes of Health (NIH) grants HL140836, HL142650, and HL126141. Dr Karki is supported by NIH K01 grant DK114897. Dr Farb is supported by NIH K23 grant HL135394. Dr Gower is supported by CTSA (Clinical and Translational Science Award) grant 1UL1TR001430. Dr Walsh is supported by NIH grant HL142650 and HL131006.

## Disclosures

None.

## Supplemental Material

Supplementary excel files I and II.

## REFERENCES

- Neeland IJ, Poirier P, Després JP. Cardiovascular and metabolic heterogeneity of obesity: clinical challenges and implications for management. *Circulation*. 2018;137:1391–1406. doi: 10.1161/CIRCULATIONAHA.117.029617
- Farb MG, Gokce N. Visceral adiposopathy: a vascular perspective. *Horm Mol Biol Clin Invest*. 2015;21:125–136. doi: 10.1515/hmbci-2014-0047
- Ahmadieh S, Kim HW, Weintraub NL. Potential role of perivascular adipose tissue in modulating atherosclerosis. *Clin Sci (Lond)*. 2020;134:3–13. doi: 10.1042/CS20190577
- Ozen G, Daci A, Norel X, Topal G. Human perivascular adipose tissue dysfunction as a cause of vascular disease: focus on vascular tone and wall remodeling. *Eur J Pharmacol*. 2015;766:16–24. doi: 10.1016/j.ejphar.2015.09.012
- Antoniadou C, Antonopoulos AS, Deanfield J. Imaging residual inflammatory cardiovascular risk. *Eur Heart J*. 2020;41:748–758. doi: 10.1093/eurheartj/ehz474
- Fitzgibbons TP, Czech MP. Epicardial and perivascular adipose tissues and their influence on cardiovascular disease: basic mechanisms and clinical associations. *J Am Heart Assoc*. 2014;3:e000582. doi: 10.1161/JAHA.113.000582
- Galarraga M, Campión J, Muñoz-Barrutia A, Boqué N, Moreno H, Martínez JA, Milagro F, Ortiz-de-Solórzano C. Adiposoft: automated software for the analysis of white adipose tissue cellularity in histological sections. *J Lipid Res*. 2012;53:2791–2796. doi: 10.1194/jlr.D023788
- Gensini GG. A more meaningful scoring system for determining the severity of coronary heart disease. *Am J Cardiol*. 1983;51:606. doi: 10.1016/s0002-9149(83)80105-2
- Rampidis GP, Benetos G, Benz DC, Giannopoulos AA, Buechel RR. A guide for Gensini Score calculation. *Atherosclerosis*. 2019;287:181–183. doi: 10.1016/j.atherosclerosis.2019.05.012
- Fuster JJ, Ouchi N, Gokce N, Walsh K. Obesity-induced changes in adipose tissue microenvironment and their impact on cardiovascular disease. *Circ Res*. 2016;118:1786–1807. doi: 10.1161/CIRCRESAHA.115.306885
- Zuriaga MA, Fuster JJ, Farb MG, MacLauchlan S, Bretón-Romero R, Karki S, Hess DT, Apovian CM, Hamburg NM, Gokce N, et al. Activation of non-canonical WNT signaling in human visceral adipose tissue contributes to local and systemic inflammation. *Sci Rep*. 2017;7:17326. doi: 10.1038/s41598-017-17509-5
- Bettini S, Favaretto F, Compagnin C, Belligoli A, Sanna M, Fabris R, Serra R, Dal Prà C, Prevedello L, Foletto M, et al. Resting energy expenditure, insulin resistance and UCP1 expression in human subcutaneous and visceral adipose tissue of patients with obesity. *Front Endocrinol (Lausanne)*. 2019;10:548. doi: 10.3389/fendo.2019.00548
- Zuriaga MA, Fuster JJ, Gokce N, Walsh K. Humans and mice display opposing patterns of “browning” gene expression in visceral and subcutaneous white adipose tissue depots. *Front Cardiovasc Med*. 2017;4:27. doi: 10.3389/fcvm.2017.00027
- Libby P, Hansson GK. From focal lipid storage to systemic inflammation: JACC review topic of the week. *J Am Coll Cardiol*. 2019;74:1594–1607. doi: 10.1016/j.jacc.2019.07.061
- Watts SW, Gollasch M. Perivascular adipose tissue (PVAT) in health and disease. *Front Physiol*. 2018;9:1004.
- Scott SS, Yang X, Robich M, Liaw L, Boucher JM. Differentiation capacity of human aortic perivascular adipose progenitor cells. *J Vis Exp*. 2019;145:10.3791/59337. doi: 10.3791/59337
- Rajsheker S, Manka D, Blomkalns AL, Chatterjee TK, Stoll LL, Weintraub NL. Crosstalk between perivascular adipose tissue and blood vessels. *Curr Opin Pharmacol*. 2010;10:191–196. doi: 10.1016/j.coph.2009.11.005
- Watts SW, Flood ED, Garver H, Fink GD, Roccabianca S. A new function for perivascular adipose tissue (PVAT): assistance of arterial stress relaxation. *Sci Rep*. 2020;10:1807. doi: 10.1038/s41598-020-58368-x
- Costa RM, Neves KB, Tostes RC, Lobato NS. Perivascular adipose tissue as a relevant fat depot for cardiovascular risk in obesity. *Front Physiol*. 2018;9:253. doi: 10.3389/fphys.2018.00253
- Moos MP, John N, Gräbner R, Nossmann S, Günther B, Vollandt R, Funk CD, Kaiser B, Habenicht AJ. The lamina adventitia is the major site of immune cell accumulation in standard chow-fed apolipoprotein

- E-deficient mice. *Arterioscler Thromb Vasc Biol.* 2005;25:2386–2391. doi: 10.1161/01.ATV.0000187470.31662.f6
21. Chatterjee TK, Aronow BJ, Tong WS, Manka D, Tang Y, Bogdanov VY, Unruh D, Blomkalns AL, Piegore MG Jr, Weintraub DS, et al. Human coronary artery perivascular adipocytes overexpress genes responsible for regulating vascular morphology, inflammation, and hemostasis. *Physiol Genomics.* 2013;45:697–709. doi: 10.1152/physiolgenomics.00042.2013
  22. Verhagen SN, Vink A, van der Graaf Y, Visseren FL. Coronary perivascular adipose tissue characteristics are related to atherosclerotic plaque size and composition. A post-mortem study. *Atherosclerosis.* 2012;225:99–104. doi: 10.1016/j.atherosclerosis.2012.08.031
  23. Maiellaro K, Taylor WR. The role of the adventitia in vascular inflammation. *Cardiovasc Res.* 2007;75:640–648. doi: 10.1016/j.cardiores.2007.06.023
  24. van Hinsbergh VW, Eringa EC, Daemen MJ. Neovascularization of the atherosclerotic plaque: interplay between atherosclerotic lesion, adventitia-derived microvessels and perivascular fat. *Curr Opin Lipidol.* 2015;26:405–411. doi: 10.1097/MOL.0000000000000210
  25. Nosalski R, Guzik TJ. Perivascular adipose tissue inflammation in vascular disease. *Br J Pharmacol.* 2017;174:3496–3513. doi: 10.1111/bph.13705
  26. Verloren S, Dubrovskaya G, Tsang SY, Essin K, Luft FC, Huang Y, Gollasch M. Visceral periaortic adipose tissue regulates arterial tone of mesenteric arteries. *Hypertension.* 2004;44:271–276. doi: 10.1161/01.HYP.0000140058.28994.ec
  27. Henrichot E, Juge-Aubry CE, Pernin A, Pache JC, Velebit V, Dayer JM, Meda P, Chizzolini C, Meier CA. Production of chemokines by perivascular adipose tissue: a role in the pathogenesis of atherosclerosis? *Arterioscler Thromb Vasc Biol.* 2005;25:2594–2599. doi: 10.1161/01.ATV.0000188508.40052.35
  28. Öhman MK, Luo W, Wang H, Guo C, Abdallah W, Russo HM, Eitzman DT. Perivascular visceral adipose tissue induces atherosclerosis in apolipoprotein E deficient mice. *Atherosclerosis.* 2011;219:33–39. doi: 10.1016/j.atherosclerosis.2011.07.012
  29. Manka D, Chatterjee TK, Stoll LL, Basford JE, Konanah ES, Srinivasan R, Bogdanov VY, Tang Y, Blomkalns AL, Hui DY, et al. Transplanted perivascular adipose tissue accelerates injury-induced neointimal hyperplasia: role of monocyte chemoattractant protein-1. *Arterioscler Thromb Vasc Biol.* 2014;34:1723–1730. doi: 10.1161/ATVBAHA.114.303983
  30. Mahabadi AA, Reinsch N, Lehmann N, Altenbernd J, Kälisch H, Seibel RM, Erbel R, Möhlenkamp S. Association of pericoronary fat volume with atherosclerotic plaque burden in the underlying coronary artery: a segment analysis. *Atherosclerosis.* 2010;211:195–199. doi: 10.1016/j.atherosclerosis.2010.02.013
  31. Lehman SJ, Massaro JM, Schlett CL, O'Donnell CJ, Hoffmann U, Fox CS. Peri-aortic fat, cardiovascular disease risk factors, and aortic calcification: the Framingham Heart Study. *Atherosclerosis.* 2010;210:656–661. doi: 10.1016/j.atherosclerosis.2010.01.007
  32. Mazurek T, Zhang L, Zalewski A, Mannion JD, Diehl JT, Arafat H, Sarov-Blat L, O'Brien S, Keiper EA, Johnson AG, et al. Human epicardial adipose tissue is a source of inflammatory mediators. *Circulation.* 2003;108:2460–2466. doi: 10.1161/01.CIR.0000099542.57313.C5
  33. Gaborit B, Venticlef N, Ancel P, Pelloux V, Gariboldi V, Leprince P, Amour J, Hatem SN, Jouve E, Dutoir A, et al. Human epicardial adipose tissue has a specific transcriptomic signature depending on its anatomical peri-atrial, peri-ventricular, or peri-coronary location. *Cardiovasc Res.* 2015;108:62–73. doi: 10.1093/cvr/cvz008
  34. Baker AR, Silva NF, Quinn DW, Harte AL, Pagano D, Bonser RS, Kumar S, McTernan PG. Human epicardial adipose tissue expresses a pathogenic profile of adipocytokines in patients with cardiovascular disease. *Cardiovasc Diabetol.* 2006;5:1. doi: 10.1186/1475-2840-5-1
  35. Verhagen SN, Buijsrogge MP, Vink A, van Herwerden LA, van der Graaf Y, Visseren FL. Secretion of adipocytokines by perivascular adipose tissue near stenotic and non-stenotic coronary artery segments in patients undergoing CABG. *Atherosclerosis.* 2014;233:242–247. doi: 10.1016/j.atherosclerosis.2013.12.005
  36. Oikonomou EK, Marwan M, Desai MY, Mancio J, Alashi A, Hutt Centeno E, Thomas S, Herdman L, Kotanidis CP, Thomas KE, et al. Non-invasive detection of coronary inflammation using computed tomography and prediction of residual cardiovascular risk (the CRISP CT study): a post-hoc analysis of prospective outcome data. *Lancet.* 2018;392:929–939. doi: 10.1016/S0140-6736(18)31114-0
  37. Ohyama K, Matsumoto Y, Takanami K, Ota H, Nishimiya K, Sugisawa J, Tsuchiya S, Amamizu H, Uzuka H, Suda A, et al. Coronary adventitial and perivascular adipose tissue inflammation in patients with vasospastic angina. *J Am Coll Cardiol.* 2018;71:414–425. doi: 10.1016/j.jacc.2017.11.046
  38. Sims FH. A comparison of coronary and internal mammary arteries and implications of the results in the etiology of arteriosclerosis. *Am Heart J.* 1983;105:560–566. doi: 10.1016/0002-8703(83)90478-7
  39. Chatterjee TK, Stoll LL, Denning GM, Harrelson A, Blomkalns AL, Idelman G, Rothenberg FG, Neltner B, Romig-Martin SA, Dickson EW, et al. Proinflammatory phenotype of perivascular adipocytes: influence of high-fat feeding. *Circ Res.* 2009;104:541–549. doi: 10.1161/CIRCRESAHA.108.182998
  40. Ferrari G, Quackenbush J, Strobeck J, Hu L, Johnson CK, Mak A, Shaw RE, Sayles K, Brizzio ME, Zapolanski A, et al. Comparative genome-wide transcriptional analysis of human left and right internal mammary arteries. *Genomics.* 2014;104:36–44. doi: 10.1016/j.ygeno.2014.04.005
  41. Drosos I, Chalikias G, Pavlaki M, Kareli D, Epitropou G, Bougioukas G, Mikroulis D, Konstantinou F, Giatromanolaki A, Ritis K, et al. Differences between perivascular adipose tissue surrounding the heart and the internal mammary artery: possible role for the leptin-inflammation-fibrosis-hypoxia axis. *Clin Res Cardiol.* 2016;105:887–900. doi: 10.1007/s00392-016-0996-7
  42. Numaguchi R, Furuhashi M, Matsumoto M, Sato H, Yanase Y, Kuroda Y, Harada R, Ito T, Higashiura Y, Koyama M, et al. Differential phenotypes in perivascular adipose tissue surrounding the internal thoracic artery and diseased coronary artery. *J Am Heart Assoc.* 2019;8:e011147. doi: 10.1161/JAHA.118.011147
  43. Malinowski M, Deja MA, Janusiewicz P, Golba KS, Roleder T, Wos S. Mechanisms of vasodilatory effect of perivascular tissue of human internal thoracic artery. *J Physiol Pharmacol.* 2013;64:309–316.
  44. He GW, Fan L, Grove KL, Furnary A, Yang Q. Expression and function of endothelial nitric oxide synthase messenger RNA and protein are higher in internal mammary than in radial arteries. *Ann Thorac Surg.* 2011;92:845–850. doi: 10.1016/j.athoracsurg.2011.04.063
  45. Gimbrone MA Jr, Topper JN, Nagel T, Anderson KR, Garcia-Cardena G. Endothelial dysfunction, hemodynamic forces, and atherogenesis. *Ann N Y Acad Sci.* 2000;902:230–9; discussion 239. doi: 10.1111/j.1749-6632.2000.tb06318.x
  46. Tarr FI, Sasvári M, Tarr M, Rácz R. Evidence of nitric oxide produced by the internal mammary artery graft in venous drainage of the recipient coronary artery. *Ann Thorac Surg.* 2005;80:1728–1731. doi: 10.1016/j.athoracsurg.2005.05.005
  47. Lebona GT. Morphological variations of the human ascending aortic fold. *J Anat.* 1993;182(Pt 2):275–279.
  48. Karastergiou K, Evans I, Ogston N, Miheisi N, Nair D, Kaski JC, Jahangiri M, Mohamed-Ali V. Epicardial adipokines in obesity and coronary artery disease induce atherogenic changes in monocytes and endothelial cells. *Arterioscler Thromb Vasc Biol.* 2010;30:1340–1346. doi: 10.1161/ATVBAHA.110.204719
  49. Shibasaki I, Nishikimi T, Mochizuki Y, Yamada Y, Yoshitatsu M, Inoue Y, Kuwata T, Ogawa H, Tsuchiya G, Ishimitsu T, et al. Greater expression of inflammatory cytokines, adrenomedullin, and natriuretic peptide receptor-C in epicardial adipose tissue in coronary artery disease. *Regul Pept.* 2010;165:210–217. doi: 10.1016/j.regpep.2010.07.169
  50. Iacobellis G, Pistilli D, Gucciardo M, Leonetti F, Miraldi F, Brancaccio G, Gallo P, di Gioia CR. Adiponectin expression in human epicardial adipose tissue in vivo is lower in patients with coronary artery disease. *Cytokine.* 2005;29:251–255. doi: 10.1016/j.cyt.2004.11.002
  51. Fitzgibbons TP, Lee N, Tran KV, Nicoloso S, Kelly M, Tam SK, Czech MP. Coronary disease is not associated with robust alterations in inflammatory gene expression in human epicardial fat. *JCI Insight.* 2019;4:e124859.
  52. Sacks HS, Fain JN, Holman B, Cheema P, Chary A, Parks F, Karas J, Optican R, Bahouth SW, Garrett E, et al. Uncoupling protein-1 and related messenger ribonucleic acids in human epicardial and other adipose tissues: epicardial fat functioning as brown fat. *J Clin Endocrinol Metab.* 2009;94:3611–3615. doi: 10.1210/jc.2009-0571
  53. Akoumianakis I, Sanna F, Margaritis M, Badi I, Akawi N, Herdman L, Coutinho P, Fagan H, Antonopoulos AS, Oikonomou EK, et al. Adipose tissue-derived WNT5A regulates vascular redox signaling in obesity via USP17/RAC1-mediated activation of NADPH oxidases. *Sci Transl Med.* 2019;11:eaav5055.
  54. Owen MK, Witzmann FA, McKenney ML, Lai X, Berwick ZC, Moberly SP, Alloosh M, Sturek M, Tune JD. Perivascular adipose tissue potentiates contraction of coronary vascular smooth muscle: influence of obesity. *Circulation.* 2013;128:9–18. doi: 10.1161/CIRCULATIONAHA.112.001238
  55. Greenstein AS, Khavandi K, Withers SB, Sonoyama K, Clancy O, Jeziorska M, Laing I, Yates AP, Pemberton PW, Malik RA, et al.

Local inflammation and hypoxia abolish the protective anticontractile properties of perivascular fat in obese patients. *Circulation*. 2009;119:1661–1670. doi: 10.1161/CIRCULATIONAHA.108.821181

56. Meijer RI, Bakker W, Alta CL, Sipkema P, Yudkin JS, Viollet B, Richter EA, Smulders YM, van Hinsbergh VW, Serné EH, et al. Perivascular adipose tissue control of insulin-induced vasoreactivity in muscle is impaired in db/db mice. *Diabetes*. 2013;62:590–598. doi: 10.2337/db11-1603
57. Sacks HS, Fain JN. Human epicardial adipose tissue: a review. *Am Heart J*. 2007;153:907–917. doi: 10.1016/j.ahj.2007.03.019
58. Rosito GA, Massaro JM, Hoffmann U, Ruberg FL, Mahabadi AA, Vasan RS, O'Donnell CJ, Fox CS. Pericardial fat, visceral abdominal fat, cardiovascular disease risk factors, and vascular calcification in a community-based sample: the Framingham Heart Study. *Circulation*. 2008;117:605–613. doi: 10.1161/CIRCULATIONAHA.107.743062
59. Britton KA, Wang N, Palmisano J, Corsini E, Schlett CL, Hoffmann U, Larson MG, Vasan RS, Vita JA, Mitchell GF, et al. Thoracic periaortic and visceral adipose tissue and their cross-sectional associations with measures of vascular function. *Obesity (Silver Spring)*. 2013;21:1496–1503. doi: 10.1002/oby.20166
60. Ishii T, Asuwa N, Masuda S, Ishikawa Y. The effects of a myocardial bridge on coronary atherosclerosis and ischaemia. *J Pathol*. 1998;185:4–9. doi: 10.1002/(SICI)1096-9896(199805)185:1<4::AID-PATH50>3.0.CO;2-3
61. Ketonen J, Shi J, Martonen E, Mervaala E. Periadventitial adipose tissue promotes endothelial dysfunction via oxidative stress in diet-induced obese C57Bl/6 mice. *Circ J*. 2010;74:1479–1487. doi: 10.1253/circj.09-0661
62. Li X, Ballantyne LL, Yu Y, Funk CD. Perivascular adipose tissue-derived extracellular vesicle miR-221-3p mediates vascular remodeling. *FASEB J*. 2019;33:12704–12722. doi: 10.1096/fj.201901548R
63. Farb MG, Karki S, Park SY, Saggese SM, Carmine B, Hess DT, Apovian C, Fetterman JL, Bretón-Romero R, Hamburg NM, et al. WNT5A-JNK regulation of vascular insulin resistance in human obesity. *Vasc Med*. 2016;21:489–496. doi: 10.1177/1358863X16666693
64. Karki S, Ngo DTM, Farb MG, Park SY, Saggese SM, Hamburg NM, Carmine B, Hess DT, Walsh K, Gokce N. WNT5A regulates adipose tissue angiogenesis via anti-Angiogenic VEGFA165b in obese humans. *Am J Physiol Heart Circ Physiol*. 2017;313:H200–H206.
65. Withers SB, Agabiti-Rosei C, Livingstone DM, Little MC, Aslam R, Malik RA, Heagerty AM. Macrophage activation is responsible for loss of anticontractile function in inflamed perivascular fat. *Arterioscler Thromb Vasc Biol*. 2011;31:908–913. doi: 10.1161/ATVBAHA.110.221705
66. Aghamohammadzadeh R, Greenstein AS, Yadav R, Jeziorska M, Hama S, Soltani F, Pemberton PW, Ammorì B, Malik RA, Soran H, et al. Effects of bariatric surgery on human small artery function: evidence for reduction in perivascular adipocyte inflammation, and the restoration of normal anticontractile activity despite persistent obesity. *J Am Coll Cardiol*. 2013;62:128–135. doi: 10.1016/j.jacc.2013.04.027
67. Zeng ZH, Zhang ZH, Luo BH, He WK, Liang LY, He CC, Su CJ. The functional changes of the perivascular adipose tissue in spontaneously hypertensive rats and the effects of atorvastatin therapy. *Clin Exp Hypertens*. 2009;31:355–363. doi: 10.1080/10641960902977916